SUPPLEMENT

EXPLAINING EXTREME EVENTS OF 2016 FROM A CLIMATE PERSPECTIVE

Editors
Stephanie C. Herring, Nikolaos Christidis, Andrew Hoell, James P. Kossin,
Carl J. Schreck III, and Peter A. Stott

Special Electronic Supplement to the
Bulletin of the American Meteorological Society
Vol. 99, No. 1, January 2018

Cover credits:
©The Ocean Agency / XL Catlin Seaview Survey / Chrisophe Bailhache—A panoramic image of coral bleaching at Lizard Island on the Great Barrier Reef, captured by The Ocean Agency / XL Catlin Seaview Survey / Christophe Bailhache in March 2016.

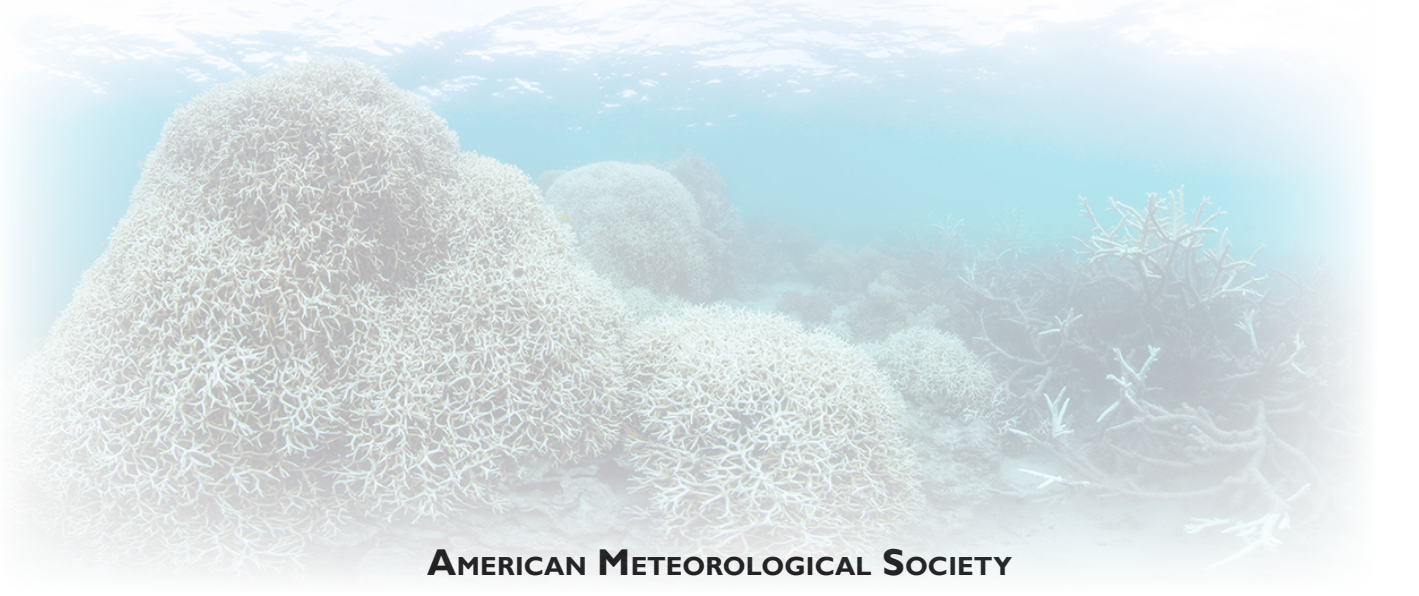

AMERICAN METEOROLOGICAL SOCIETY

ES12. ANTHROPOGENIC FORCINGS AND ASSOCIATED CHANGES IN FIRE RISK IN WESTERN NORTH AMERICA AND AUSTRALIA DURING 2015/16

Simon F. B. Tett, Alexander Falk, Megan Rogers, Fiona Spuler, Calum Turner, Joshua Wainwright, Oscar Dimdore-Miles, Sam Knight, Nicolas Freychet, Michael J. Mineter, and Caroline E. R. Lehmann

This document is a supplement to "Anthropogenic Forcings and Associated Changes in Fire Risk in Western North America and Australia during 2015/16," by Simon F. B. Tett, Alexander Falk, Megan Rogers, Fiona Spuler, Calum Turner, Joshua Wainwright, Oscar Dimdore-Miles, Sam Knight, Nicolas Freychet, Michael J. Mineter, and Caroline E. R. Lehmann (*Bull. Amer. Meteor. Soc.*, **99** (1), S60–S64) • ©2018 American Meteorological Society • DOI:10.1175/BAMS-D-17-0096.2

Construction of natural sea surface temperatures and sea ice concentrations.

The sea surface temperatures (SST) and sea ice concentrations (SIC) were constructed following Stone (2013). SST was estimated by taking the difference in seasonally varying monthly mean skin temperature from 19 climate models submitted to the CMIP5 project (Taylor et al. 2012) between 51 simulations run under the RCP4.5 scenario and 51 simulations run under the "historicalNat" scenario; this attributable warming estimate is then subtracted from the observed SST. SIC is adjusted for consistency with the cooler SST through a modified version of the algorithm used in Pall et al (2011). The effect of this on SST for the period September 2015 to August 2016 shows a cooling of about 0.75°C in the tropics, about 0.5°C in the midlatitudes, and cooling of more than 1°C in the equatorial Pacific (Fig. ES12.1a).

Drivers of VPD change.

In the main text we computed VPD as

$$V = k\, q\, p^* \left(\frac{1}{RH} - 1\right)$$

where

$$k = \frac{M_{dry\ air}}{M_{H_2O}} = 1.60677214.$$ q/RH is q_s (the saturated humidity) so:

$$V = k q_s\, p^* \,(1 - RH) \qquad \text{Eqn S1.}$$

q_s is a function of atmospheric temperature and surface pressure. As changes in temperature have been attributed on continental scales to human influences, and changes in p^* are likely small, we have more confidence in changes that are driven by q_s rather than other variables. Partitioning all variables into a mean value, which we define as the masked area-averaged normals from the **Historical** ensemble and a change defined as the masked area-averaged monthly average anomalies we can write Eqn. S1 as:

$$\bar{V} + V' = (\overline{q_s} + q_s')\,(\overline{p^*} + p^{*\prime})\,(1 - (\overline{RH} + RH'))/k\,.$$

Rearranging and removing the $\bar{V}$ term we obtain:

$$V' = q_s'\,\overline{p^*}\,\frac{(1-\overline{RH})}{k} + \overline{q_s}\,p^{*\prime}\frac{1-\overline{RH}}{k} - \overline{q_s}\,\overline{p^*}\frac{RH'}{k} + r\,.$$

Where r is a residual representing 2nd and higher order terms computed from the difference between V' and the sum of the first three terms.

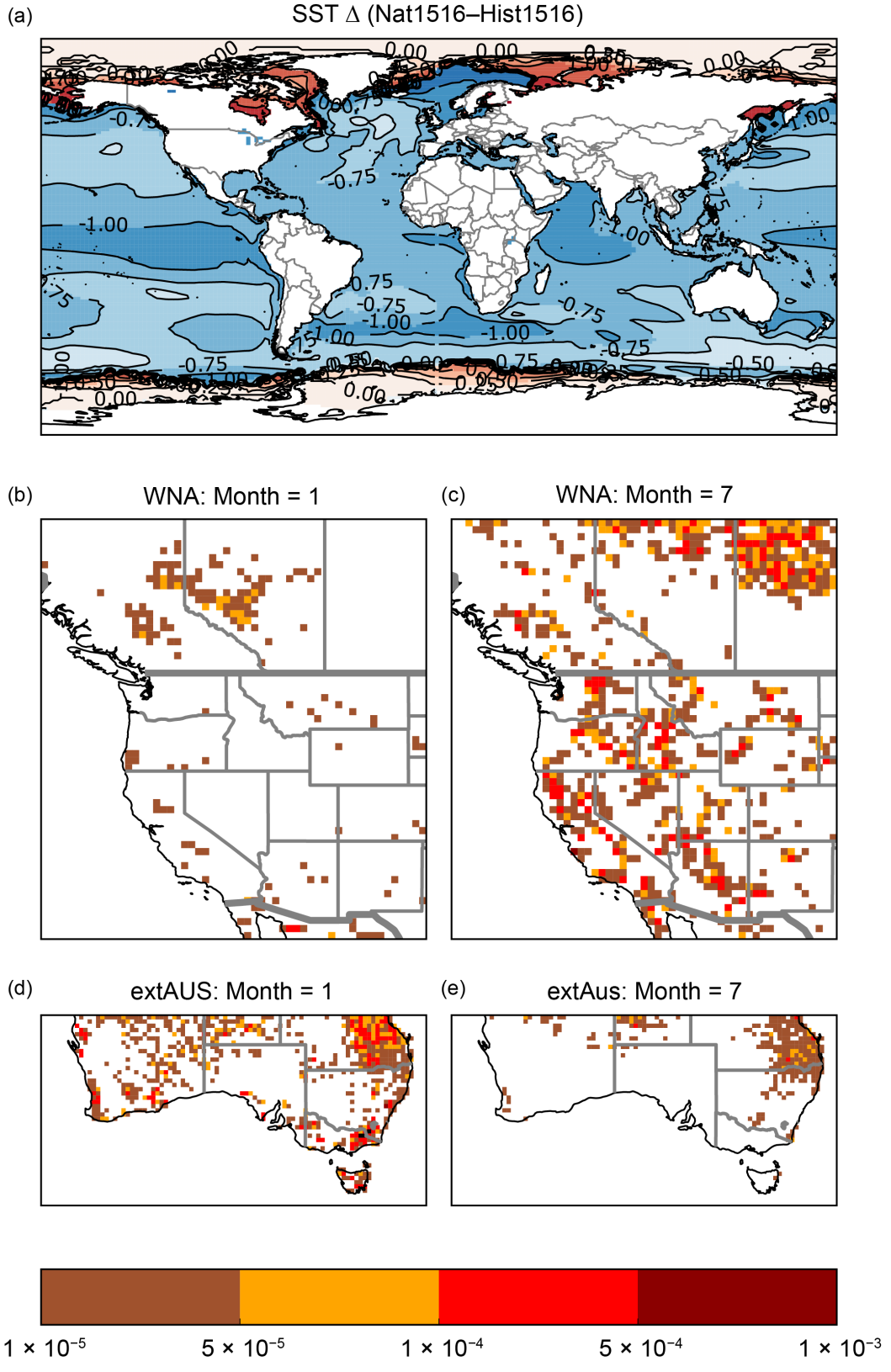

Fig. ES12.1. (a) SST difference (°C) between Nat15–16 and Hist15–16. Contours are every 0.25°C between −1 and +1. Fraction of pixels (2003–16) with fire detected by MODIS on *Aqua* for Jan (b),(d) and Jul (c),(e). (b),(c) Shows WNA region; (d),(e) shows extAUS region.

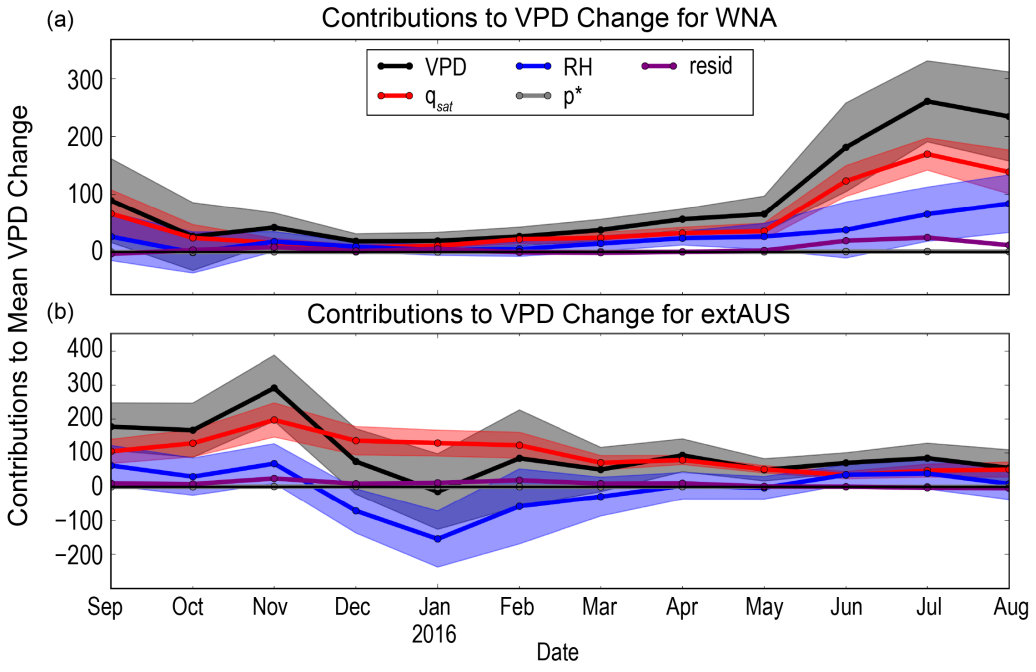

Fig. ES12.2. Average contributions to VPD (black) difference between Hist15–16 and Nat15–16 ensembles from changes in saturated humidity (red), relative humidity (blue), surface pressure (gray), and residual (purple) changes. (a) Shows changes for WNA; (b) shows changes for extAUS. Shading around VPD, saturated humidity, and relative humidity shows the 2σ uncertainty in the mean ensemble differences computed by bootstrapping.

REFERENCES

Pall, P., T. Aina, D. A. Stone, P. A. Stott, T. Nozawa, A. G. J. Hilberts, D. Lohmann, and M. R. Allen, 2011: Anthropogenic greenhouse gas contribution to flood risk in England and Wales in autumn 2000. *Nature*, **470**, 382–385, doi:10.1038/nature09762.

Stone, D. A., 2013: Boundary conditions for the C20C Detection and Attribution project: The All-Hist/est1 and Nat-Hist/CMIP5-est1 scenarios. International CLIVAR C20C+ Detection and Attribution Project, 18 pp. (Available online at http://portal.nersc.gov/c20c/input_data/C20C-DandA_dSSTs_All-Hist-est1_Nat-Hist-CMIP5-est1.pdf.)

Taylor, K. E., R. J. Stouffer, and G. A. Meehl, 2012: An overview of CMIP5 and the experiment design. *Bull. Amer. Meteor. Soc.*, **93**, 485–498, doi:10.1175/BAMS-D-00094.1.